Optimizing control of simulated moving bed separations of mixtures subject to the generalized Langmuir isotherm

Author(s):
Grossmann, Christian; Amanullah, Mohammad; Morari, Manfred; Mazzotti, Marco; Morbidelli, Massimo

Publication date:
2008

Permanent link:
https://doi.org/10.3929/ethz-b-000012515

Originally published in:
Adsorption 14(2-3), https://doi.org/10.1007/s10450-007-9083-8

Adsorption (2008) 14: 423–432
DOI 10.1007/s10450-007-9083-8

Optimizing control of simulated moving bed separations of mixtures subject to the generalized Langmuir isotherm

Cristian Grossmann · Mohammad Amanullah · Manfred Morari · Marco Mazzotti · Massimo Morbidelli

Received: 25 April 2007 / Revised: 5 November 2007 / Accepted: 19 November 2007 / Published online: 4 December 2007

Abstract Simulated moving bed (SMB) is a cost-efficient separation technique that offers high productivity and low solvent consumption. SMB has gained importance in the pharmaceutical and fine chemical industry to perform complex separation tasks. However, an open and challenging problem is the optimal, robust operation of the SMB process. We have developed a control scheme that integrates the optimization and control of the SMB unit. A significant feature of the controller is that only minimal information of the system has to be provided, i.e. the linear adsorption behavior of the mixture to be separated and the average void fraction of the columns. Therefore, a full characterization of the adsorption behavior of the mixture and the columns is no longer required. In this 'cycle to cycle' control scheme, the measurements, optimization and control actions are performed once in every cycle. This paper presents simulation results of the control scheme applied to the separation of binary mixtures characterized by generalized Langmuir isotherms. The results are presented and analyzed in the frame of the triangle theory that has been recently extended to encompass these types of isotherms. Besides, online optimum performance of the SMB unit is compared with off-line optimization carried out using genetic algorithm. The results show that the controller fulfills the product and process specifications while operating the SMB unit optimally, regardless of the different types of Langmuir isotherms that the systems exhibit.

Keywords Multicolumn processes · Preparative chromatography · Liquid phase adsorption

C. Grossmann · M. Morari (✉)
Automatic Control Laboratory, ETH Zurich, 8092 Zurich, Switzerland
e-mail: morari@control.ee.ethz.ch

M. Amanullah · M. Mazzotti
Institute of Process Engineering, ETH Zurich, 8092 Zurich, Switzerland

M. Mazzotti
e-mail: marco.mazzotti@ipe.mavt.ethz.ch

M. Morbidelli
Institute for Chemical and Bio-Engineering, ETH Zurich, 8092 Zurich, Switzerland

1 Introduction

This paper addresses the question whether the optimizing controller of Simulated Moving Beds (SMBs) that has been developed in our group in the last few years works effectively whatever the nonlinear isotherm, which the species to be separated are subject to. The optimizing controller is based only on information about the linear retention behavior of the species to be separated (Abel et al. 2004; Erdem et al. 2004a), but it has been proved to be effective in the control of the SMB separation of species subject to the Langmuir isotherm (Erdem et al. 2004b). The effectiveness of the controller has been demonstrated also experimentally, on systems subject to a linear (Abel et al. 2005; Erdem et al. 2005, 2006) and to a Langmuir isotherm (Amanullah et al. 2007). More recently the controller has been extended to the so-called 'cycle to cycle' control and new capabilities, e.g. the possibility of varying the switch time during operation, have been added (Amanullah et al. 2007; Grossmann et al. 2007, 2008).

As far as the controller performance is concerned, this paper aims at bridging the gap between the Langmuir isotherm and any other nonlinear isotherms. This is an important is-

sue, since a controller whose operation is based on only data about the linear retention behavior of the species to be separated, i.e. under dilute conditions, and whose performance is the same whatever the underlying nonlinear isotherm would represent a major step forward in the potential and application of SMB, particularly for pharmaceutical applications and chiral separations. This would allow in fact avoiding the lengthy and cumbersome determination of the adsorption isotherm and operating an SMB unit for a new separation in a very short time.

This is important because the SMB technology has gained attention in the fast growing field of chiral and pharmaceutical products where time to market rather than economics of the separation is the decisive criterion (Francotte and Richert 1997). During early drug development phases, only limited amount of the mixture to be separated is available and pure components might not even be accessible at all. Therefore, strong performance determining factors like solid and mobile phases have to be selected with some screening criteria. As a result, the design and optimization of a new chiral SMB separation is often based on a trade-off between accuracy in the system parameters and heuristic search of feasible operating conditions. A number of literature contributions have been devoted to prove SMB's feasibility for chiral (Negawa and Shoji 1992; Ching et al. 1993; Nicoud et al. 1993; Charton and Nicoud 1995; Küsters et al. 1995; Cavoy et al. 1997; Guest 1997; Pais et al. 1997; Schulte et al. 1997; Juza et al. 1998; Nagamatsu et al. 1999; Pedeferri et al. 1999) and fine chemical separations (Gattuso et al. 1996; Gottschlich et al. 1996; Gottschlich and Kashe 1997; Yun et al. 1997; Wu et al. 1998), as well as to show how SMB separations can be developed quickly using small amount of material for the initial characterization (Francotte and Richert 1997; Guest 1997; Francotte et al. 1998; Heuer et al. 1998; James et al. 1999). Besides, efforts and advances have been made on the theoretical side, i.e. in the field of process optimization. On the one hand, powerful and straightforward short-cut design methods like the triangle theory (Mazzotti et al. 1997) have been developed using simplified SMB dynamics, i.e. the equilibrium model that neglects mass transfer and axial dispersion effects. On the other hand, advanced numerical optimization techniques have been applied and adapted to SMB processes (Kawajiri and Biegler 2006a, 2006b, 2006c). These approaches can handle efficiently more and more detailed models of the SMB dynamics that account for mass transfer, axial dispersion and diffusion within the particle pores. Nevertheless, as the optimization techniques become more detailed, the need for accurate system parameters increases and might become a limiting factor. In such a context it is rather evident that the controller we have developed, when applicable to any type of isotherms, would represent a very significant asset for SMB practitioners.

A powerful, though simple, model to capture a large variety of different nonlinear retention behaviors, including different combinations of adsorption and desorption composition fronts, is provided by the generalized Langmuir isotherms (Mazzotti 2006c). These are four different isotherms, for which in the case of binary systems and in the frame of the equilibrium theory of nonlinear chromatography it has been possible to derive exact criteria for complete separation in a SMB, i.e. the so called triangle theory (Mazzotti 2006a, 2006b). This is very practical in the context of our study since it allows for a deeper understanding of the controller's behavior and for a direct comparison between the operating conditions predicted by the triangle theory and achieved by the controller.

The paper is organized as follows: in Sect. 2, a brief overview of the SMB process, generalized Langmuir isotherms, control concepts and optimization problems are presented. In Sect. 3, the performance of the controller for the separation of mixtures characterized by generalized Langmuir isotherms is assessed and discussed.

2 Background

2.1 Process

A detailed description of the SMB process and its working principle may be found elsewhere (Mazzotti et al. 1997; Erdem et al. 2004b; Grossmann et al. 2008) and only a short summary is given here.

Four different binary mixtures are to be separated in a closed-loop four-section eight-column SMB unit arranged in a 2-2-2-2 configuration. The SMB unit is operated in standard isocratic mode. The feed concentration of the mixtures to be separated is reported in Table 1, whereas the characteristics of the SMB unit are summarized in Table 2.

The retention behavior of the species to be separated is described by the following generalized Langmuir isotherm (Mazzotti 2006c):

$$n_i = \frac{H_i c_i}{1 + p_1 K_1 c_1 + p_2 K_2 c_2}, \quad i = 1,\ 2 \tag{1}$$

where n_i and c_i are the fluid and adsorbed phase concentrations, respectively; H_i and K_i are the Henry and equilibrium constants for component i, respectively. Component 2 is assumed to be more retained than component 1, i.e. $H_2 > H_1$. The parameters p_1 and p_2 can take the values ± 1, and their combination characterizes the retention behavior of the four binary mixtures to be separated as shown in Table 1. The first mixture, indicated in the following as mixture L, is described by setting $p_1 = p_2 = 1$, which corresponds to the well-known Langmuir isotherm. When $p_1 = p_2 = -1$ an

Table 1 Isotherm parameters of the four mixtures to be separated

Type of isotherm (mixture)	p_1	p_2	H_1	H_2	$K_1 = K_2$ [L/g]	$c_1^f = c_2^f$ [g/L]
Langmuir (L)	1	1	1	2	0.1	1.5
Anti-Langmuir (A)	−1	−1	1	2	0.1	1.5
Mixed Langmuir (M_1)	1	−1	1	2	0.1	1.5
Mixed Langmuir (M_2)	−1	1	1	2	0.1	1.5

Table 2 Physical parameters of the SMB unit used for simulation

Parameter	Value
Number of columns	8
Column distribution	2/2/2/2 closed loop
Column diameter	1 cm
Column length	10 cm
Total packing porosity	$\varepsilon = 0.4$
Theoretical plates per column	100
Switch time	$t^* = 120$ s

Anti-Langmuir isotherm is obtained for mixture A. The remaining two mixtures, M_1 and M_2, are described by setting $p_1 = 1 = -p_2$ and $p_1 = -1 = -p_2$, respectively. It is worth noting that not all fluid phase concentrations are allowed since the denominator in (1) has to remain positive for any non-negative pair (c_1, c_2). For instance, considering the allowed feed concentrations of our mixtures, where $c_1^f = c_2^f$ in all cases, the following inequality has to hold:

$$1 + p_1 K_1 c_1^f + p_2 K_2 c_2^f > 0 \tag{2}$$

This constraint is redundant in the Langmuir case. However, in the other three cases it poses an additional constraint to the positive orthant of the (c_1, c_2) plane for the allowed feed concentrations. For a detailed discussion about the physical consistency of the generalized Langmuir isotherm please refer to (Mazzotti 2006c).

Note that according to the (1) the behavior of the four mixtures under dilute conditions reduces to the same linear behavior, i.e. $n_i = H_i c_i$ for small c_i, with the same values of the Henry constants. Since the controller uses the values of the Henry constants only, this implies that exactly the same controller with exactly the same parameters is used to control the SMB separation of all four binary mixtures.

2.2 Control concept

At the core of our control approach there is the integration of the optimization and control of the SMB unit. The controller makes use of the four internal flow rates, $Q_1, \ldots, Q_4$, as manipulated variables to drive the unit to an operating point that fulfills the product and process specifications while optimizing an objective function. Note that in this work the switch time t^* of the unit remains constant throughout the operation although it is possible to extend the controller to include t^* among the manipulated variables (Grossmann et al. 2007). The decisions on how to operate the unit are taken on the basis of the measurements from the plant, i.e. the feedback information. The average concentration of component 1 and 2 in the extract and raffinate streams over one cycle, $c_{1,ave}^E$, $c_{2,ave}^E$, $c_{1,ave}^R$ and $c_{2,ave}^R$, represent the feedback information. Collecting this type of information implies waiting one complete cycle to get each measurement. The sampling rate is then chosen to be equal to the cycle time, therefore, the measurements, optimization and control actions are performed only once every cycle, i.e. on a 'cycle to cycle' basis (Grossmann et al. 2008).

The control problem to be solved at every cycle is formulated as a constrained dynamic optimization problem within the repetitive model predictive control (RMPC) framework (Natarajan and Lee 2000). We provide objectives and specifications to the controller in the form of a cost function and of constraints for the optimization problem. The productivity and solvent consumption contribute to the cost function to be optimized, whereas the product quality specifications and the operational restrictions of the plant are imposed as constraints. The controller makes use of a simplified 'cycle to cycle' SMB model to predict and optimize the performance of the unit over a predefined number of cycles, n_p, i.e. the so-called prediction horizon. The solution of the optimization problem yields a sequence of optimal control actions for a chosen number of cycles, namely the control horizon, n_c. This is implemented according to a receding horizon strategy, i.e. the first element of the calculated optimal control actions sequence corresponding to the current cycle is implemented, and the remaining calculated optimal inputs are discarded. The prediction horizon is shifted by one cycle and as new measurements of the average concentrations of both species in extract and raffinate are available, an optimization problem based on the new estimate of the plant state is solved. The new state estimate is calculated using a Kalman filter.

A significant feature of the controller is that the simplified 'cycle to cycle' SMB model used by the controller requires only the linear isotherm information, i.e. H_1 and H_2, and the average bed porosity of the unit, ε_{ave}. These can be easily obtained from pulse injection experiments under

dilute conditions. The solution of the optimization problem calculated at every cycle determines the dynamic behavior of the controller as well as its performance. The cost function and the optimization constraints are discussed briefly in order to highlight the performance determining factors of the controller. A detailed description of the theory behind the controller and its implementation can be found elsewhere (Amanullah et al. 2007; Grossmann et al. 2008).

2.2.1 *Online optimization*

The optimization problem is formulated as a linear program (LP), i.e. the cost function and the constraints are linear in the decision variables. In the LP to be solved at cycle k, the four internal flow rates over the control horizon n_c, $Q_j(l)$ for $j = 1, \ldots, 4$ and $l = k, \ldots, k + n_c - 1$, represent the decision variables. These are constrained by lower and upper bounds:

$$Q_j^{max} \geq Q_j(l) \geq Q_j^{min} \quad \text{for } j = 1, \ldots, 4,\ l = k, \ldots, k + n_c - 1 \tag{3}$$

In order to guarantee a smooth operation of the plant, maximum allowable flow rate changes, ΔQ_j^{max}, are imposed and formulated as inequality constraints as follows:

$$\Delta Q_j^{max} \geq |\Delta Q_j(l)| \tag{4}$$

$$s_j^{(1)} \geq |\Delta Q_j(l)| \quad \text{with } s_j^{(1)} \geq 0 \quad \text{for } j = 1, \ldots, 4,\ l = k, \ldots, k + n_c - 1 \tag{5}$$

where $\Delta Q_j(l) = Q_j(l) - Q_j(l-1)$. Inequality (5) allows minimizing the changes in the flow rates by penalizing the slack variable $s_j^{(1)}$ in the cost function (see below). A different weighting of these slack variables in the cost function allows expressing the preference for the use of one manipulated variable over another.

The required product specifications are enforced by constraining the average purity of the extract, $P_{ave}^E(l)$, and raffinate, $P_{ave}^R(l)$, stream for each cycle of the prediction horizon with lower bounds P_{min}^E and P_{min}^R, respectively. Since the internal flow rates are constant during each of the cycles, the minimum purity constraints can be expressed as:

$$P_{ave}^E(l) = \frac{c_{1,ave}^E(l)}{c_{1,ave}^E(l) + c_{2,ave}^E(l)} \geq P_{min}^E - s^{(2)} \quad \text{with } s^{(2)} \geq 0 \tag{6}$$

$$P_{ave}^R(l) = \frac{c_{2,ave}^R(l)}{c_{1,ave}^R(l) + c_{2,ave}^R(l)} \geq P_{min}^R - s^{(3)} \quad \text{with } s^{(3)} \geq 0 \text{ for } l = k+1, \ldots, k+n_p \tag{7}$$

The parameters $s^{(2)}$ and $s^{(3)}$ are slack variables that allow softening the constraints and guaranteeing feasibility; they are highly penalized in the cost function. Note that $P_{ave}^E(l)$ and $P_{ave}^R(l)$ for $l = k+1, \ldots, k+n_p$ are nonlinear functions of the concentrations and have to be linearized in order to be compatible with the LP formulation. These can then be computed from the estimation of the plant state obtained from the measurements and the Kalman filter. The optimization problem is defined as follows, where the quantity to be minimized is the cost function:

$$\min_{\mathbf{Q}_j^{n_c},\, \mathbf{S}} \sum_{l=k}^{k+n_c-1} \lambda_D \underbrace{Q_D(l)}_{Q_1(l)-Q_4(l)} - \lambda_F \underbrace{Q_F(l)}_{Q_3(l)-Q_2(l)} + \lambda_{\mathbf{s}^{(1)}} \mathbf{s}^{(1)} + \lambda_{s^{(2)}} s^{(2)} + \lambda_{s^{(3)}} s^{(3)} \tag{8}$$

$\mathbf{Q}_j^{n_c}$ is a vector comprising the flow rates for the control horizon n_c; $\mathbf{S}$ is a vector containing the slack variables used to soften the constraints; Q_F and Q_D are the feed and desorbent flow rates to be maximized and minimized, respectively, over a given control horizon n_c; λ_D and λ_F are the weighting factors to reflect the relative importance given to the desorbent consumption minimization and the productivity or feed throughput maximization, respectively. The row vector $\lambda_{\mathbf{s}^{(1)}}$ contains the weight for each of the slack variables $s_j^{(1)}$, i.e. the elements of the column vector $\mathbf{s}^{(1)}$. The parameters $\lambda_{s^{(2)}}$ and $\lambda_{s^{(3)}}$ are the weights for the slack variables used in the purity constraints defined by (6) and (7).

There are four objectives reflected in the cost function that will guide the controller's behavior. The first and second terms express the objective of maximizing the productivity and minimizing the desorbent consumption, respectively. The third term makes the controller try to minimize the changes of the flow rates. Finally, the last two terms express the objectives of minimizing the extent of softening of the purity constraints and therefore allowing off-spec production.

In a real SMB operation, the weights of the terms in the cost function of (8) depend on the specific features of the separation and reflect the target product's value and the separation costs. The behavior of the controller depends on the choice of the weights, which in this work are such as to maximize productivity and minimize off-spec production. Furthermore, the controller tries to minimize the desorbent consumption as long as this does not conflict with the other two main objectives. This is reflected in the numerical values of the parameters used for the simulation that are reported in Table 3.

The set of inequality constraints (3)–(7) and the cost function (8) complete the formulation of the LP. The problem comprises 300 variables, and 367 constraints. A commercial solver, ILOG CPLEX 7.0 was used to solve the optimization problem. The maximum computation time was found to be less than 0.1 s in a PC with a 3 GHz processor.

Table 3 The parameters used for the implementation of the controller. All the flow rate parameters are given in [mL/min]

Parameter	Value
Q_1^{max}	10.00
Q_2^{max}	7.00
Q_3^{max}	9.30
Q_4^{max}	7.00
Q_j^{min} for $j = 1, \ldots, 4$	0.60
ΔQ_j^{max} for $j = 1, \ldots, 4$	0.12
$P_{min}^E = P_{min}^R$	99.0%
λ_F	20
λ_D	2
$\lambda_{\mathbf{s}^{(1)}}$	[4000 400 400 4000]
$\lambda_{s^{(2)}} = \lambda_{s^{(3)}}$	100
n_c	1 cycle
n_p	8 cycles

Table 4 Objective function, decision variables, and constraints for the off-line optimization using genetic algorithm

Objective function	minimize: $\lambda_D Q_D - \lambda_F Q_F$
Decision variables	Q_j for $j = 1, \ldots, 4$
Constraints	$P_{min}^E = P_{min}^R = 99.0\%$; $t^* = 120$ s

2.3 Off-line optimization

The performance obtained with the controller was compared with those attained through off-line optimization. To allow for fair comparison, comparable objective function and constraints were defined, as reported in Table 3. The cost function, decision variables and constraints for the off-line optimization are reported in Table 4. Note that at steady state, the slack variables in (8) are all zero. Hence they are not included in the objective function of the off-line optimization. The objective function, while represents performance index, reflects in a quantitative manner the performance of the SMB process and is used as the basis for the comparison of the online and the off-line optimizations.

A non-sorting genetic algorithm (NSGA) is used as optimization algorithm, whose detailed description may be found elsewhere (Zhang et al. 2003).

3 Results

This section is devoted to the implementation of the control concept presented in Sect. 2.2 on the virtual SMB plant described in Sect. 2.1. The goal is to demonstrate that supplying the Henry constants and the average porosity of the SMB columns to the model of the controller is adequate to meet the process and product specifications and to operate the unit optimally whatever the nonlinear isotherm characterizing the mixture to be separated.

The results are analyzed using the so-called triangle theory (Mazzotti et al. 1997, Mazzotti 2006a, 2006b). For the sake of completeness, the main concepts are summarized here. The separating conditions are derived on the basis of the equilibrium theory model. The five operating parameters of the SMB, i.e. the four sectional flow rates and the switch time, are combined into four dimensionless sectional flow rate ratios that characterize the performance of the unit:

$$m_j = \frac{Q_j t^* - V\varepsilon}{V(1-\varepsilon)} \quad (j = 1, \ldots, 4) \tag{9}$$

Note that the flow rate ratios m_j are linear functions of the flow rates when the switch time t^* is fixed; V is the volume of one column and ε is the total packing porosity. The necessary and sufficient conditions for the complete separation of any system can be cast in the general form:

$$m_{1,min} < m_1 \tag{10}$$

$$m_{2,min} < m_2 < m_{2,max} \tag{11}$$

$$m_{3,min} < m_3 < m_{3,max} \tag{12}$$

$$m_4 < m_{4,max} \tag{13}$$

The upper and lower bounds for the sectional flow rate ratios depend on the specific isotherm and on its parameters. They are given as functions of m_2, m_3, the adsorption isotherm parameters and the feed composition. A detailed analysis, derivation and description of these bounds may be found elsewhere (Mazzotti 2006a, 2006b). The separation conditions can be graphically represented in two different plots. The first one refers to the m_2 and m_3 flow rate ratios, and represent the complete separation region in the (m_2, m_3) plane; it is shown in the top left part of the regions of Figs. 1a, 2a, 3a, and 4a, since m_3 is larger than m_2 hence feasible operating points lie above the diagonal of the (m_2, m_3) plane. When the inequalities (10) and (13) are fulfilled, the position of the operating point in the (m_2, m_3) plane allows one to make a prediction of the separation performance. The triangular region defined by (11) and (12) for each mixture represents the set of operating points for which, in the frame of equilibrium theory, a complete separation of the mixture is achieved (Mazzotti 2006a, 2006b). Note that the point on the (m_2, m_3) plane that maximizes the feed throughput, which is proportional to the difference between m_3 and m_2, at complete separation is the vertex of the complete separation region.

The second plot refers to the flow rate ratios m_1 and m_4. Since $m_1 > m_4$ the corresponding complete separation region defined by (10) and (13) is below the diagonal of the plane of horizontal coordinate m_1 and of vertical coordinate

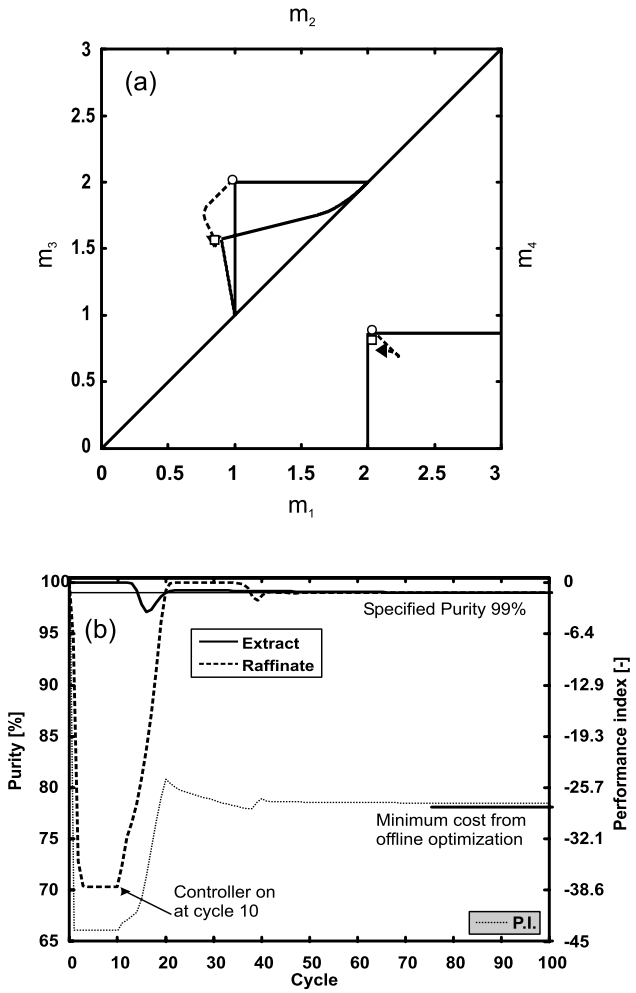

Fig. 1 Langmuir isotherm: (**a**) trajectory of the operation for the separation of mixture L. *Upper left*: (m_2, m_3) plane. *Lower right*: (m_1, m_4) plane. *Symbols*; ○: startup point, ►: final operating point, □: optimum found through off-line optimization. (**b**): purity of the product streams and performance index during the controlled SMB operation

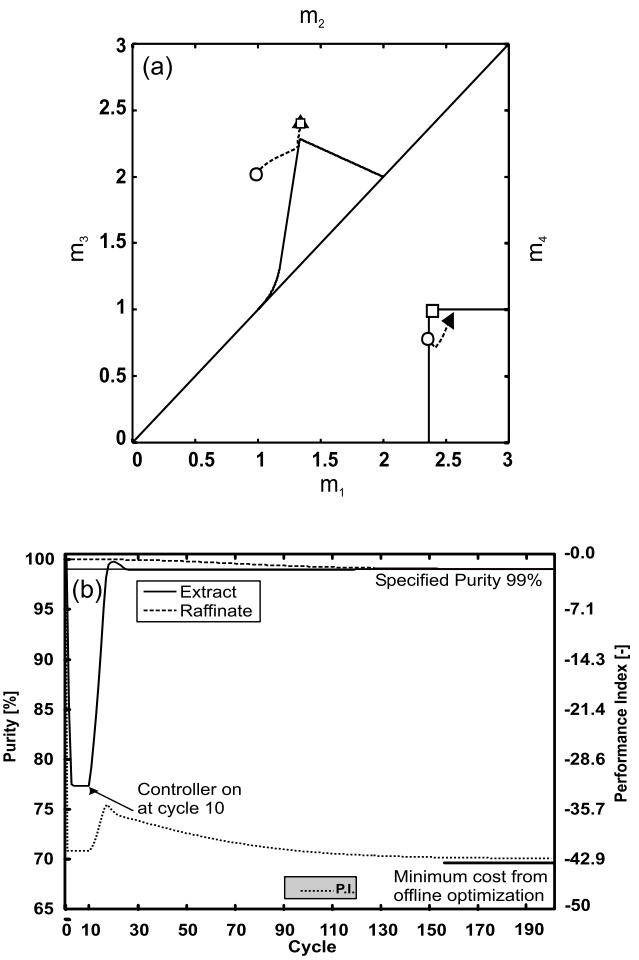

Fig. 2 Anti-Langmuir isotherm: (**a**) trajectory of the operation for the separation of mixture A. *Upper left*: (m_2, m_3) plane. *Lower right*: (m_1, m_4) plane. *Symbols*; ○: startup point, ►: final operating point, □: optimum found through off-line optimization. (**b**): purity of the product streams and performance index during the controlled SMB operation

m_4 (see the lower right part of Figs. 1a, 2a, 3a, and 4a). Fulfilling the constraints of (10) and (13) implies that the solvent is fully regenerated when leaving section 4 and being recycled to section 1, and that the adsorbent in section 1 is fully regenerated too. Since these constraints depend on m_2 and m_3 the values in the figures have been calculated using the optimal operating point calculated through off-line optimization.

To assess the performance of the controller, all four generalized Langmuir isotherms have been studied. In all cases, the same controller, and only the linear adsorption isotherm information, are used to carry out the separation of the binary mixtures characterized by the isotherms reported in Table 1 in an SMB featuring the characteristics given in Table 2. All four operations have been carried out with initially clean columns and from the initial operating point as given in Table 5. The feed concentration of the two species to be separated is in all four cases $c_1^f = c_2^f = 1.5$ g/L. The complete separation regions in the operating parameter space in the four cases depend on the feed composition, as well as on the isotherm parameters, and are plotted in Figs. 1a, 2a, 3a, and 4a. The controller is switched on at cycle 10 with the aim of fulfilling the process and product specifications and of optimizing the performance of the unit. It is worth emphasizing here again that the controller has no information about what adsorption isotherm the mixture to be separated is subject to. Only the feedback information from the plant gives insight about to what extent and in which direction the product purities deviate from the set points. Based on the feedback, on the embedded simplified model of the SMB and on the optimization problem the controller is able to decide how to correct the operating conditions in all four cases.

Figures 1b, 2b, 3b, and 4b show the evolution of the product purities and of the performance indices with re-

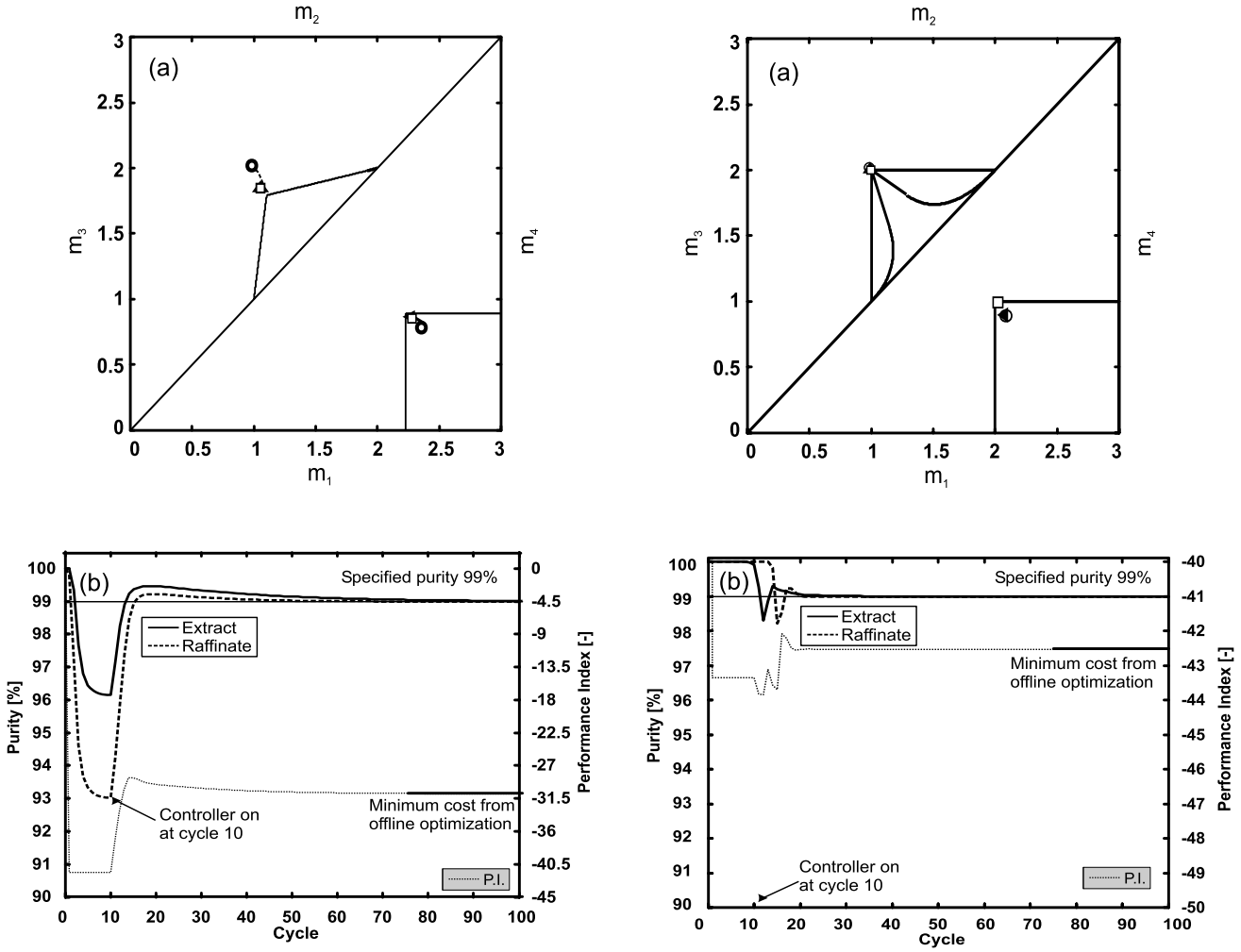

Fig. 3 Mixed type 1 (M_1) isotherm: (**a**) trajectory of the operation for the separation of mixture M_1. *Upper left*: (m_2, m_3) plane. *Lower right*: (m_1, m_4) plane. *Symbols*; ○: startup point, ►: final operating point, □: optimum found through off-line optimization. (**b**): purity of the product streams and performance index during the controlled SMB operation

Fig. 4 Mixed type 2 (M_2) isotherm: (**a**) trajectory of the operation for the separation of mixture M_2. *Upper left*: (m_2, m_3) plane. *Lower right*: (m_1, m_4) plane. *Symbols*; ○: startup point, ►: final operating point, □: optimum found through off-line optimization. (**b**): purity of the product streams and performance index during the controlled SMB operation

spect to time (units are the number of cycles, a cycle being the time needed to switch the SMB inlet and outlet ports a number of times equal to the number of columns in the unit). We observe that the required purity specifications of 99.0% for both the extract and raffinate streams are fulfilled in all cases. However, the time needed to fulfill the purity requirements is different for the four different cases (L: 45, A: 130, M_1: 80, M_2: 25 cycles). This is because of the different dynamics of the SMB process in the case of different isotherms characterizing the mixture to be separated and of the different relative position of the initial operating point with respect to the optimal operating point achieved by the controller. In all cases, a quicker fulfillment of the purity requirements is followed by a slower optimization. This behavior is a direct consequence of the way the weights in the cost function have been chosen.

Table 5 Start-up flow rates (mL/min)

Flow rates	L	A	M_1	M_2
Q_1	6.34	7.11	7.11	6.48
Q_2	3.88	3.88	3.88	3.88
Q_3	6.33	6.33	6.33	6.33
Q_4	3.66	3.42	3.42	3.66

The violation of the purity constraints is heavily penalized in the cost function and therefore these requirements are quickly fulfilled at the beginning of the operation. During the rest of the operation the controller aims at maximizing the feed throughput, of course, without violating the purity constraints, which gives rise to the rather slow and cautious optimization.

Table 6 Flow rates and performance indices obtained for four different mixtures from the 'cycle to cycle' online optimizing control runs (c2c) and the off-line genetic algorithm optimization (Off-line)

Flow rates [mL/min]	L		A		M_1		M_2	
	c2c	Off-line	c2c	Off-line	c2c	Off-line	c2c	Off-line
Q_1	6.54	6.34	7.52	7.21	6.91	6.93	6.45	6.34
Q_2	3.55	3.56	4.73	4.73	4.05	4.05	3.89	3.91
Q_3	5.26	5.26	7.24	7.22	5.92	5.93	6.30	6.28
Q_4	3.31	3.48	3.72	3.91	3.60	3.57	3.68	3.90
PI [−]	−27.7	−28.2	−42.7	−43.3	−30.7	−30.8	−42.5	−42.5
$\triangle Q_F$	−0.6%		−0.8%		+0.5%		−1.3%	
$\triangle Q_D$	−12.9%		−15.2%		+1.5%		−13.5%	

The trajectories of the operating points in the operating parameter space are shown in Figs. 1a, 2a, 3a, and 4a. The values of the flow rates attained by the controller at steady state are reported in Table 6, together with the corresponding values calculated by off-line optimization. Note that in all cases, the final operating point in the (m_2, m_3) plane are located near the vertex of the corresponding regions of complete separation. Note that in the case of the mixed Langmuir isotherm M_2, the initial operating point is by chance very close to the optimal operating point in the (m_2, m_3) plane.

On the contrary, the final operating points in the (m_1, m_4) plane are not optimal as they are close to neither the vertex of the complete separation region predicted by triangle theory nor the optimal point calculated by off-line optimization. This is reflected by the larger amount of desorbent used by the controller than required compared to the off-line optimization (see Table 6). Such behavior of the controller is due to the presence of the slack variables in the cost function of (8). These variables help to guide and define the behavior of the controller during the transient periods, i.e. while the flow rates are being manipulated. The weights $\lambda_{\mathbf{s}^{(1)}}$ on the slack variables define how much and which flow rate is preferably used for control purposes. In our study, we preferred manipulating the flow rates in the sections 2 and 3 rather than the ones in sections 1 and 4 ($\lambda_{\mathbf{s}^{(1)}} = [4000\ 400\ 400\ 4000]$), which is also consistent with our objective of maximizing the feed throughput ($\lambda_F = 20$) more than of minimizing the desorbent consumption ($\lambda_D = 2$). On the other hand, $\lambda_{s^{(2)}}$ and $\lambda_{s^{(3)}}$ define how fast we would like to achieve the specified purities or to minimize the off-spec production, which is in our case the first priority ($\lambda_{s^{(2)}} = \lambda_{s^{(3)}} = 100$). The weights we have chosen are effective in allowing for the feed throughput maximization and the minimization of the off-spec production by fulfilling the specified purities relatively quickly, but they are apparently less effective in minimizing the desorbent consumption. If priorities were different, the weights could be tuned accordingly.

4 Concluding remarks

The analysis and results presented in this paper prove that the SMB optimizing controller that our group has developed over the last few years is capable of controlling and optimizing SMB operation for systems subject to any type of generalized Langmuir isotherms. The controller uses the same set of minimal information, namely the behavior of the components to be separated in the linear range, i.e. at high dilution, in all four cases of generalized Langmuir isotherms. Since these four isotherms cover a range of retention behaviors that is rather broad, we argue that the optimizing controller will be able to control and to optimize SMB operation for systems subject to any isotherm based on information about the retention behavior of the species to be separated under very dilute conditions only. This capability of the controller makes it virtually no more necessary the costly and lengthy determination of adsorption isotherms during the development of a new SMB separation. Based on the experience that we have gained in transferring the controller from a virtual to a real, experimental environment in the case of the linear and Langmuir isotherms, we are confident that also in the case of the other three isotherms discussed in this work the experimental performance of the controller will be similar to the one obtained in simulations.

As far as the optimizing capabilities of the controller are concerned, we have compared the separation performance attained by the online controller and those achievable as calculated through off-line optimization. The two compares very well, in terms of feed throughput, with the online optimizer. However, the online optimizing controller is less ef-

fective in minimizing desorbent consumption. An explanation for such behavior, based on the choice of the weighting factors in the cost function used by the controller, has been presented and discussed. As to the dynamic behavior of the controller, we have noted differences among the four generalized Langmuir isotherms that deserve further study in order to ascertain whether these differences stem from the choice of the tuning parameters or of the initial operating point, which is obviously in a different position with respect to the final optimal operating point.

Acknowledgements We thank ETH research commission for partially funding this work through project number TH-19/03-3.

References

Abel, S., Erdem, G., Mazzotti, M., Morari, M., Morbidelli, M.: Optimizing control of simulated moving beds—linear isotherm. J. Chromatogr. A **1033**, 229–239 (2004)

Abel, S., Erdem, G., Amanullah, M., Morari, M., Mazzotti, M., Morbidelli, M.: Optimizing control of simulated moving beds—experimental implementation. J. Chromatogr. A **1092**, 2–16 (2005)

Amanullah, M., Grossmann, C., Morari, M., Mazzotti, M., Morbidelli, M.: Experimental implementation of automatic 'cycle to cycle' control of simulated moving beds: chiral separation. J. Chromatogr. A **1165**, 100–108 (2007)

Cavoy, E., Deltent, M.F., Lehoucq, S., Miggiano, D.: Laboratory-developed simulated moving bed for chiral drug separations. Design of the system and separation of Tramadol enantiomers. J. Chromatogr. A **769**, 49–57 (1997)

Charton, F., Nicoud, R.M.: Complete design of a simulated moving bed. J. Chromatogr. A **702**, 97–112 (1995)

Ching, C.B., Lim, B.G., Lee, E.J.D., Ng, S.C.: Preparative resolution of praziquantel enantiomers by simulated counter-current chromatography. J. Chromatogr. A **634**, 215–219 (1993)

Erdem, G., Abel, S., Morari, M., Mazzotti, M., Morbidelli, M.: Automatic control of simulated moving beds—II: nonlinear isotherm. Ind. Eng. Chem. Res. **43**, 3895–3907 (2004a)

Erdem, G., Abel, S., Morari, M., Mazzotti, M., Morbidelli, M., Lee, J.H.: Automatic control of simulated moving beds. Ind. Eng. Chem. Res. **43**, 405–421 (2004b)

Erdem, G., Abel, S., Amanullah, M., Morari, M., Mazzotti, M., Morbidelli, M.: Automatic control of simulated moving beds—experimental verification. Adsorption **11**, 573–577 (2005)

Erdem, G., Amanullah, M., Morari, M., Mazzotti, M., Morbidelli, M.: Optimizing control of an experimental simulated moving bed unit. AIChE J. **52**, 1481–1494 (2006)

Francotte, E., Richert, J.: Application of simulated moving bed chromatography to the separation of the enantiomers of chiral drugs. J. Chromatogr. A **769**, 101–107 (1997)

Francotte, E., Richert, J., Mazzotti, M., Morbidelli, M.: Simulated moving bed chromatographic resolution of a chiral antitussive. J. Chromatogr. A **796**, 239–248 (1998)

Gattuso, M., McCulloch, B., Priegnitz, J.: Simulated moving bed technology for cost-effective chiral products. Chem. Tech. Eur. **3**, 27 (1996)

Gottschlich, N., Kashe, V.: Purification of monoclonal antibodies by simulated moving-bed chromatography. J. Chromatogr. A **765**, 201 (1997)

Gottschlich, N., Weidgen, S., Kashe, V.: Continuous biospecific affinity purification of enzymes by simulated moving bed chromatography. Theoretical description and experimental results. J. Chromatogr. A **719**, 267–274 (1996)

Grossmann, C., Amanullah, M., Mazzotti, M., Morbidelli, M., Morari, M.: Optimizing control of variable cycle time simulated moving beds. In: IFAC 8th International Symposium on Dynamics and Control of Process Systems, Cancun, Mexico, No. 225 (2007)

Grossmann, C., Amanullah, M., Morari, M., Mazzotti, M., Morbidelli, M.: Cycle to cycle optimizing control of simulated moving beds. AIChE J. **54**, 194–208 (2008)

Guest, D.W.: Evaluation of simulated moving bed chromatography for pharmaceutical process development. J. Chromatogr. A **760**, 159–162 (1997)

Heuer, C., Küsters, E., Plattner, T., Seidel-Morgenstern, A.: Design of the simulated moving bed process based on adsorption isotherm measurements using a perturbation method. J. Chromatogr. A **827**, 175 (1998)

James, F., Sepulveda, M., Charton, F., Quinones, I., Guiochon, G.: Determination of binary competitive equilibrium isotherms from the individual chromatographic band profiles. Chem. Eng. Sci. **54**, 1677 (1999)

Juza, M., Di Giovanni, O., Biressi, G., Mazzotti, M., Schurig, V., Morbidelli, M.: Continuous enantiomer separation of the volatile inhalation anesthetic enflurane with a gas chromatographic simulated moving bed (GC-SMB) unit. J. Chromatogr. A **813**, 333–347 (1998)

Kawajiri, Y., Biegler, L.: Large scale nonlinear optimization for asymmetric operation and design of simulated moving beds. J. Chromatogr. A **1133**, 226–240 (2006a)

Kawajiri, Y., Biegler, L.: A nonlinear programming superstructure for optimal dynamic operations of simulated moving processes. Ind. Eng. Chem. Res. **45**(25), 8503–8513 (2006b)

Kawajiri, Y., Biegler, L.: Optimization Strategies for simulated moving bed and powerfeed processes. AIChE J. **52**(4), 1343–1350 (2006c)

Küsters, E., Gerber, G., Antia, F.D.: Enantioseparation of a chiral epoxide by simulated moving bed chromatography using Chiralcel-OD. Chromatographia **40**, 387–393 (1995)

Mazzotti, M.: Design of simulated moving bed separations: generalized Langmuir isotherm. Ind. Eng. Chem. Res. **45**, 6311–6324 (2006a)

Mazzotti, M.: Equilibrium theory based design of simulated moving bed processes for a generalized Langmuir isotherm. J. Chromatogr. A **1126**, 311–322 (2006b)

Mazzotti, M.: Local equilibrium theory for the binary chromatography of species subject to a generalized Langmuir isotherm. Ind. Eng. Chem. Res. **45**, 5332–5350 (2006c)

Mazzotti, M., Storti, G., Morbidelli, M.: Optimal operation of simulated moving bed units for nonlinear chromatographic separations. J. Chromatogr. A **769**, 3–24 (1997)

Nagamatsu, S., Murazumi, K., Makino, S.: Chiral separation of a pharmaceutical intermediate by a simulated moving bed process. J. Chromatogr. A **832**, 55 (1999)

Natarajan, S., Lee, J.: Repetitive model predictive control applied to a simulated moving bed chromatography system. Comput. Chem. Eng. **24**, 1127–1133 (2000)

Negawa, M., Shoji, F.: Optical resolution by simulated moving bed adsorption technology. J. Chromatogr. A **590**, 113–117 (1992)

Nicoud, R.M., Fuchs, G., Adam, P., Bailly, M., Küsters, E., Antia, F.D., Reuille, R., Schmid, E.: Preparative scale enantioseparation of a chiral epoxide: comparison of liquid chromatography and simulated moving bed adsorption technology. Chirality **5**, 267 (1993)

Pais, L.S., Loureiro, J.M., Rodrigues, A.E.: Separation of 1-1′-bi-2-naphthol enantiomers by continuous chromatography in simulated moving bed. Chem. Eng. Sci. **52**, 245–257 (1997)

Pedeferri, M., Zenoni, G., Mazzotti, M., Morbidelli, M.: Experimental analysis of a chiral separation through simulated moving bed chromatography. Chem. Eng. Sci. **54**, 3735–3748 (1999)

Schulte, M., Ditz, R., Devant, R.M., Kinkel, J., Charton, F.: Comparison of the specific productivity of different chiral stationary phases used for simulated moving bed chromatography. J. Chromatogr. A **769**, 93 (1997)

Wu, D.-J., Xie, Y., Ma, Z., Wang, N.-H.L.: Design of simulated moving bed chromatography for amino acid separations. Ind. Eng. Chem. Res. **37**, 4023–4035 (1998)

Yun, T., Zhong, G., Guiochon, G.: Experimental study of the influence of the flow rated in SMB chromatography. AIChE J. **43**, 2970 (1997)

Zhang, Z., Mazzotti, M., Morbidelli, M.: Multiobjective optimization of simulated moving bed and VARICOL processes using a genetic algorithm. J. Chromatogr. A **989**, 95–108 (2003)